Bioorganic & Medicinal Chemistry 27 (2019) 383–393

Contents lists available at ScienceDirect

Bioorganic & Medicinal Chemistry

journal homepage: www.elsevier.com/locate/bmc

Design, synthesis, and biological evaluation of radioiodinated benzo[*d*]imidazole-quinoline derivatives for platelet-derived growth factor receptor β (PDGFRβ) imaging

Nurmaya Effendi[a,b,g], Kenji Mishiro[c,g], Takeshi Takarada[d], Daisuke Yamada[d], Ryuichi Nishii[e], Kazuhiro Shiba[f], Seigo Kinuya[a], Akira Odani[a], Kazuma Ogawa[a,c,*]

[a] *Graduate School of Medical Sciences, Kanazawa University, Kanazawa 920-1192, Japan*
[b] *Faculty of Pharmacy, Universitas Muslim Indonesia, Makassar 90-231, Indonesia*
[c] *Institute for Frontier Science Initiative, Kanazawa University, Kanazawa 920-1192, Japan*
[d] *Graduate School of Medicine, Dentistry and Pharmaceutical Sciences, Okayama University, Okayama 700-8558, Japan*
[e] *Department of Molecular Imaging and Theranostics, National Institute of Radiological Sciences (NIRS), QST, Inage-ku, Chiba 263-8555, Japan*
[f] *Advanced Science Research Centre, Kanazawa University, Kanazawa 920-8640, Japan*

ARTICLE INFO

Keywords:
Radioligand
Molecular imaging
PDGFRβ
Tyrosine kinase inhibitor

ABSTRACT

Several malignant tumors and fibrotic diseases are associated with PDGFRβ overexpression and excessive signaling, making this receptor attractive for molecular targeting and imaging approaches. A series of benzo[*d*]imidazole-quinoline derivatives were designed and synthesized to develop radioiodinated compounds as PDGFRβ-specific imaging probes. The structure activity relationship (SAR) evaluation of the designed compounds was performed. Among them, 2-[5-(2-methoxyethoxy)-1*H*-benzo[*d*]imidazol-1-yl]-8-(piperazin-1-yl) quinoline (**5a**) and 4-{2-[5-(2-methoxyethoxy)-1*H*-benzo[*d*]imidazol-1-yl]quinolin-8-yl}morpholine (**5d**) exhibited a relatively high PDGFRβ-TK inhibitory potency, whereas iodinated **5a** derivative 5-iodo-2-[5-(2-methoxyethoxy)-1*H*-benzo[*d*]imidazol-1-yl]-8-(piperazin-1-yl)quinoline (**8**) exhibited a superior inhibitory potency as PDGFRβ inhibitor than iodinated **5d** derivative 4-{5-iodo-2-[5-(2-methoxyethoxy)-1*H*-benzo[*d*]imidazol-1-yl]quinolin-8-yl}morpholine (**11**). Furthermore, [^{125}I]**8** and [^{125}I]**11** were synthesized and evaluated for PDGFRβ radioligand ability, both *in vitro* and *in vivo*. Cellular uptake experiments showed that [^{125}I]**8** had a higher uptake in BxPC3-luc cells as PDGFRβ-positive cells than [^{125}I]**11**. Incubation of [^{125}I]**8** after pretreatment of PDGFRβ ligands significantly reduced the uptake of [^{125}I]**8**. In biodistribution experiments using tumor-bearing mice, [^{125}I]**8** accumulation in the tumor 1 h postinjection was higher than that of the benzo[*d*]imidazol-quinoline derivative [^{125}I]IIQP, used in our previous research. These results indicate that [^{125}I]**8** could be a promising PDGFRβ imaging agent. Although its clinical application requires further structural modifications, the results obtained in this research may be useful for the development of PDGFRβ-specific radioligands.

1. Introduction

Platelet-derived growth factor receptor β (PDGFRβ) is a transmembrane receptor tyrosine kinase with highly regulated cell expression.[1] PDGFRβ exerts an important role for angiogenesis and embryonic growth, and for the formation of blood vessels, kidneys, and adipocytes.[2] In adults, PDGFRβ is expressed mainly in vascular smooth muscle cells and pericytes and its signaling is vital for wound healing and regulation of tissue interstitial fluid pressure.[3,4] Cancers are associated with aberrant expression and signaling of PDGFRβ, through autocrine and paracrine stimulation of tumor cell growth.[5,6] PDGFRβ expression by pericytes is necessary for the recruitment and integration in the wall of tumor vessels.[6–10] Therefore, PDGFRβ has raised considerable interest as an attractive target not only for anti-cancer drug discovery but also for cancer imaging.

Currently, biopsy constitutes the predominant way to determine relevant tumor molecular targets. However, a limited number of samples can be taken from a few locations, and it is associated with a certain morbidity.[11] Nuclear molecular imaging, which allows simultaneous and repeated visualization of the molecular targets

* Corresponding author at: Institute for Frontier Science Initiative, Kanazawa University, Kanazawa 920-1192, Japan.
E-mail address: kogawa@p.kanazawa-u.ac.jp (K. Ogawa).
[g] These authors contributed equally to this work.

https://doi.org/10.1016/j.bmc.2018.12.016
Received 11 September 2018; Received in revised form 7 December 2018; Accepted 10 December 2018
Available online 11 December 2018
0968-0896/

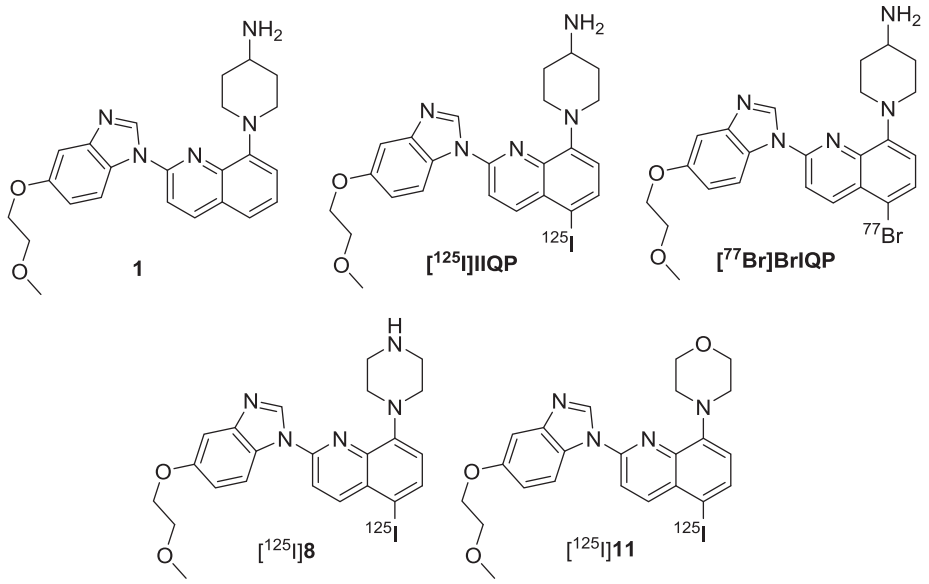

Fig. 1. Chemical structures of **1**, [^{125}I]**IIQP**, [^{77}Br]**BrIQP**, [^{125}I]**8**, and [^{125}I]**11**.

expressed in all lesions using a noninvasive procedure, could be an alternative to biopsy.[12] This allows to follow the changes in molecular target expression during the course of disease and/or in response to therapy.

In nuclear medicine, single photon emission computed tomography (SPECT) and positron emission tomography (PET) can quantify receptor density and molecular target expression.[13–15] To date, several types of probes targeting a type of receptor tyrosine kinase, such as EGFR and PDGFRβ, have been developed for cancer imaging. Some probes, which contain protein,[16,17] aptamer,[18] affibody,[19,20] or peptide[21,22] as a carrier, target extracellular domain. Some probes, which are tyrosine kinase inhibitors (TKIs) derivatives, target intracellular domains.[23–27] In this study, we designed and synthesized benzo[*d*]imidazolequinoline derivatives mimicking a PDGFRβ specific TKI as PDGFRβ imaging probes targeting intracellular domains, especially adenosine triphosphate (ATP)-binding sites. The majority of TKIs are designed to competitively bind to the ATP-binding site in the target tyrosine kinase.[28] An imaging probe mimicking a target specific TKI could be useful to select the appropriate patients and predict therapeutic effects for the original TKI. Moreover, mutation of PDGFRβ has been reported,[29,30] and the mutation status assessment by imaging with radiolabeled probes might provide valuable additional diagnostic information. In the case of other TKIs, the usefulness of imaging probes, such as assessment of drug sensitivity and mutation status, has been demonstrated. [31,32] Meanwhile, one of targets of a multikinase inhibitor sunitinib, which has been approved in the world, is the ATP-binding site in PDGFRβ.[33] It was reported that a TKI of PDGFRβ suppressed lung cancer cell proliferation,[34] and thus TKIs of PDGFRβ are anticipated to be used as anticancer agents in the future. However, imaging probes targeting the ATP-binding site of PDGFRβ has hardly been reported except our previous studies.[35,36] For the reason, we have explored the feasibilities of small molecules-based PDGFRβ imaging probes which target the ATP-binding site in intracellular domain.

In a previous study, we developed radiolabeled small molecules targeting the PDGFRβ intracellular ATP binding site, using 1-{2-[5-(2-methoxyethoxy)-1*H*-benzo[*d*]imidazol-1-yl]quinolin-8-yl}piperidin-4-amine (CP-673451, IQP, **1**), which possesses high affinity for PDGFRβ,[37] as a lead compound. [^{125}I]IIQP and [^{77}Br]BrIQP were designed, synthesized, and evaluated by introduction of radioiodine and radiobromine into **1**.[35,36] These radiolabeled probes showed high affinity for PDGFRβ and sufficient stability, both *in vitro* and *in vivo*. However, *in vivo* imaging requires higher PDGFRβ affinity and better biodistribution properties.

In order to develop more suitable radiolabeled TKIs, we investigated SAR of the substituent on the quinoline group (piperidine part) of **1**, since, to our knowledge, no reports were available on this aspect of SAR investigation and this group was easy to modify using our synthetic scheme. We designed and synthesized a new series of analogue compounds of **1** (**5a–5g** and **7a–7b**) based on the bioisosteric principle. The inhibitory effects exerted by nine compounds on PDGFRβ tyrosine kinase were evaluated using **1** as positive control. Subsequently, two new compounds with high affinity to PDFGRβ were iodinated. Using similar reagents in IIQP synthesis, 5-iodo-2-[5-(2-methoxyethoxy)-1*H*-benzo[*d*]imidazol-1-yl]-8-(piperazin-1-yl)quinoline (**8**) and 4-{5-iodo-2-[5-(2-methoxyethoxy)-1*H*-benzo[*d*]imidazol-1-yl]quinolin-8-yl}morpholine (**11**) were synthesized. The radioiodine labeled probes, [^{125}I]**8** and [^{125}I]**11** (Fig. 1), were then synthesized and evaluated *in vitro* and *in vivo* to examine their usefulness as PDGFRβ imaging probes. Although we aimed at developing probes for PET or SPECT, ^{125}I was used in the initial studies due to its longer half-life.

2. Material and methods

2.1. General

Commercial reagents and solvents were purchased from Sigma-Aldrich (St. Louis, MO, USA), Wako Pure Chemical Industries (Osaka, Japan), Nacalai Tesque, Inc., (Kyoto, Japan), Tokyo Chemical Industry, Co., Ltd., (Tokyo, Japan) and Kanto Chemical, Co., Inc. (Tokyo, Japan) and used without further purification unless otherwise stated.

[^{125}I]Sodium iodide (644 GBq/mg) was purchased from Perkin-Elmer (Waltham, MA, USA). The radioactivity was measured by an Auto Gamma System ARC-7010B (Hitachi, Ltd., Tokyo, Japan).

Bicinchoninic Acid (BCA) Protein Assay Kit and Cell Counting Kit (CCK) were purchased from Nacalai Tesque, Inc. and Dojindo (Kumamoto, Japan), respectively. Recombinant murine platelet-derived growth factor-BB (PDGF-BB) was purchased from PeproTech (Rocky Hill, NJ, USA). TR-PCT1 rodent brain pericyte cell line was a generous

gift from Dr. Emi Nakashima (Keio University, Tokyo, Japan)[38] and BxPC3-luc pancreatic cell line was purchased from JCRB Cell Bank (Ibaraki, Japan).

Proton and carbon nuclear magnetic resonance (^{1}H NMR and ^{13}C NMR) spectra were obtained with JEOL JNM-ECS400 (JEOL Ltd, Tokyo, Japan). Direct analysis in real time mass spectra (DART-MS) and Electrospray ionization mass spectra (ESI-MS) were obtained with JEOL JMS-T100TD (JEOL Ltd). Purification was conducted using reversed-phase high-performance liquid chromatography (RP-HPLC) system. TLC analysis was performed on silica plates (Art 5553, Merck, Darmstadt, Germany). Optical density in the WST-8 assay was obtained using Infinite® F200 Pro microplate reader (TECAN, Männedorf, Switzerland).

2.2. Synthesis of reference compounds and precursors

Compounds **1**, **2**, and **3** were synthesized according to our previous report.[35]

2.2.1. General procedure for the preparation of compounds (4a, 4b, 4c)

A mixture of piperazine (500 mg, 5.8 mmol, 1.0 eq.), *N,N*-diisopropylethylamine (DIPEA) (1.5 mL, 8.7 mmol, 1.5 eq.), and di-*tert*-butyl dicarbonate (Boc_2O) (500 mg, 2.3 mmol, 0.4 eq.) in dry dichloromethane (15 mL) was stirred at room temperature for 24 h under nitrogen atmosphere. The reaction mixture was diluted with dichloromethane and washed with saturated aqueous $NaHCO_3$ and brine. The organic layer was dried over anhydrous sodium sulfate, filtered, and concentrated under reduced pressure. The titled compound (**4a**) as a colorless solid was afforded after purification by column chromatography on silica gel (chloroform/methanol = 50/1). The same procedure was performed to obtain compounds **4b** and **4c**.

2.2.1.1. tert-Butyl piperazine-1-carboxylate (4a). The title compound **4a** was afforded (400 mg, 37%) as a colorless solid. ^{1}H NMR (400 MHz, $CDCl_3$): δ 1.43–1.47 (9H, br s), 1.69 (1H, s), 2.81 (4H, t, J = 5.2 Hz), 3.39 (4H, t, J = 5.2 Hz). LRMS (DART+) calcd for $C_9H_{19}N_2O_2$ [M+H$^+$]: m/z = 187.1, found 187.2.

2.2.1.2. tert-Butyl (2-aminocyclohexyl)carbamate (4b). The title compound **4b** was afforded (430 mg, 34%) as a pale yellow solid. ^{1}H NMR (400 MHz, $CDCl_3$): δ 0.88–1.04 (4H, m), 1.23–1.26 (1H, m), 1.42–1.46 (9H, br s), 1.48–1.98 (6H, m), 3.41–3.57 (1H, m), 4.54–4.58 (1H, m). LRMS (DART+) calcd for $C_{11}H_{23}N_2O_2$ [M+H$^+$]: m/z = 215.2, found 215.1.

2.2.1.3. tert-Butyl (4-aminocyclohexyl)carbamate (4c). The title compound **4c** was afforded (220 mg, 18%) as a pale yellow solid. ^{1}H NMR (400 MHz, $CDCl_3$): δ 1.15–1.25 (4H, m), 1.43–1.44 (9H, br s), 1.51 (4H, s), 1.84–1.87 (1H, m), 1.95–2.05 (2H, m), 3.39–3.49 (1H, m), 4.35–4.37 (1H, m). LRMS (DART+) calcd for $C_{11}H_{23}N_2O_2$ [M+H$^+$]: m/z = 215.2, found 215.1.

2.2.2. General procedure for the preparation of compounds (5a, 5b, 5c)

A mixture of **3** (210 mg, 0.4 mmol, 1.0 eq.), *tert*-butyl piperazine-1-carboxylate (**4a**) (150 mg, 0.8 mmol, 2.0 eq.), cesium carbonate (210 mg, 0.6 mmol, 1.5 eq.), tris(dibenzylideneacetone)dipalladium(0) (19 mg, 21 μmol, 0.05 eq.), and *rac*-BINAP (26 mg, 42 μmol, 0.1 eq.) in 1,4-dioxane (5 mL) was stirred at 100 °C for 1.5–3.5 days under nitrogen atmosphere. After removing precipitate by filtration through a pad of Celite® and washing with 1,4-dioxane, the filtrate was concentrated under reduced pressure and purified by column chromatography on silica gel (chloroform/methanol = 100/1). Trifluoroacetic acid (TFA) (1 mL) was added to purified intermediate compound and the mixture was stirred at room temperature for 15 min. After removing TFA by nitrogen gassing, the residue was dissolved in dichloromethane and washed with 0.1 M HCl. After adjusting pH to 9.0 using 0.1 M NaOH aqueous solution, the water layer was extracted using dichloromethane (3 × 25 mL). The organic layer was dried over sodium sulfate, filtered, and concentrated under reduced pressure to obtain the titled compounds (**5a**). The same procedure was carried out to obtain compounds **5b** and **5c**.

2.2.2.1. 2-[5-(2-Methoxyethoxy)-1H-benzo[d]imidazol-1-yl]-8-(piperazin-1-yl)quinoline (5a). The title compound **5a** was afforded (119 mg, 70%) as a pale yellow solid. ^{1}H NMR (400 MHz, $CDCl_3$): δ 3.29–3.30 (4H, m), 3.40–3.48 (4H, m), 3.50 (3H, s), 3.82–3.84 (2H, m), 4.23–4.25 (2H, m), 4.30–4.31 (1H, m), 7.15–7.18 (1H, m), 7.38 (1H, s), 7.49–7.54 (2H, m), 7.69–7.72 (2H, m), 8.33 (1H, d, J = 8.8 Hz), 8.46 (1H, d, J = 8.8 Hz), 8.65 (1H, s). LRMS (DART+) calcd for $C_{23}H_{26}N_5O_2$ [M+H$^+$]: m/z = 404.2, found 404.2.

2.2.2.2. (1S,2S)-N-{2-[5-(2-Methoxyethoxy)-1H-benzo[d]imidazol-1-yl]quinolin-8-yl}cyclohexane-1,2-diamine (5b). The title compound **5b** was afforded (156 mg, 86%) as a pale white solid. ^{1}H NMR (400 MHz, $CDCl_3$): δ 1.39–1.44 (4H, m), 1.55–1.61 (2H, m), 1.63–1.68 (2H, br s), 2.05–2.06 (2H, m), 2.20–2.23 (2H, m), 2.80–2.81 (1H, m), 3.20–3.30 (1H, m), 3.50 (3H, s), 3.82–3.84 (2H, m), 4.23–4.25 (2H, m), 5.82–5.91 (1H, m), 6.94 (1H, d, J = 8.0 Hz), 7.10–7.14 (2H, m), 7.39–7.43 (2H, m), 7.64 (1H, d, J = 8.8 Hz), 8.08 (1H, d, J = 9.2 Hz), 8.27 (1H, d, J = 8.8 Hz), 8.59 (1H, s). LRMS (DART+) calcd for $C_{25}H_{30}N_5O_2$ [M+H$^+$]: m/z = 432.2, found 432.3.

2.2.2.3. trans-N-{2-[5-(2-Methoxyethoxy)-1H-benzo[d]imidazole-1-yl]quinolin-8-yl}cyclohexane-1,4-diamine (5c). The title compound **5c** was afforded (148 mg, 82%) as a pale white solid. ^{1}H NMR (400 MHz, $CDCl_3$): δ 1.26–1.45 (4H, m), 1.64 (2H, br s), 1.98–2.05 (2H, m), 2.28–2.31 (2H, m), 2.80–2.82 (1H, m), 3.47–3.50 (4H, m), 3.82–3.84 (2H, m), 4.23–4.30 (2H, m), 5.82–5.90 (1H, m), 6.79 (1H, d, J = 7.6 Hz), 7.09–7.13 (2H, m), 7.39–7.43 (2H, m), 7.63 (1H, dd, J = 0.8, 8.8 Hz), 8.05 (1H, d, J = 8.8 Hz), 8.26 (1H, d, J = 9.2 Hz), 8.58 (1H, s). LRMS (DART+) calcd for $C_{25}H_{30}N_5O_2$ [M+H$^+$]: m/z = 432.2, found 432.3.

2.2.3. General procedure for the preparation of compounds (5d, 5e, 5f, 5g)

A mixture of **3** (210 mg, 0.4 mmol, 1.0 eq.), morpholine (**4d**) (70 mg, 0.8 mmol, 2.0 eq.), cesium carbonate (210 mg, 0.6 mmol, 1.5 eq.), tris(dibenzylideneacetone)dipalladium(0) (19 mg, 21 μmol, 0.05 eq.), and *rac*-BINAP (26 mg, 42 μmol, 0.1 eq.) in 1,4-dioxane (5 mL) was stirred at 100 °C for 1.5–3.5 days under nitrogen atmosphere. After removing precipitate by filtration through a pad of Celite® and washing with 1,4-dioxane, the filtrate was concentrated under reduced pressure and purified by column chromatography on silica gel (chloroform/methanol = 100/1), to obtain the titled compound (**5d**). The same procedure was carried out to obtain compounds **5e**, **5f** and **5g**.

2.2.3.1. 4-{2-[5-(2-Methoxyethoxy)-1H-benzo[d]imidazol-1-yl]quinolin-8-yl}morpholine (5d). The title compound **5d** was afforded (127 mg, 75%) as a white solid. ^{1}H NMR (400 MHz, $CDCl_3$): δ 3.43–3.45 (4H, m), 3.50 (3H, s), 3.82–3.85 (2H, m), 4.05–4.08 (4H, m), 4.23–4.25 (2H, m), 7.16 (1H, dd, J = 2.4, 8.8 Hz), 7.24–7.25 (1H, m), 7.37 (1H, d, J = 2.4 Hz), 7.48–7.54 (2H, m), 7.71 (1H, d, J = 8.8 Hz), 8.34 (1H, d, J = 9.2 Hz), 8.50 (1H, d, J = 9.2 Hz), 8.64 (1H, s). LRMS (DART+) calcd for $C_{24}H_{25}N_4O_3$ [M+H$^+$]: m/z = 405.2, found 405.2.

2.2.3.2. 2-[5-(2-Methoxyethoxy)-1H-benzo[d]imidazol-1-yl]-8-(4-methylpiperazin-1-yl)quinoline (5e). The title compound **5e** was afforded (147 mg, 84%) as a pale yellow solid. ^{1}H NMR (400 MHz,

$CDCl_3$): δ 2.48 (3H, s), 2.65–2.95 (4H, m), 3.39–3.51 (7H, m), 2.83–3.85 (2H, m), 4.21–4.25 (2H, m), 7.15–7.17 (1H, m), 7.28–7.29 (1H, m), 7.37 (1H, s), 7.47–7.53 (2H, m), 7.71 (1H, dd, J = 1.6, 8.8 Hz), 8.33 (1H, dd, J = 1.6, 8.4 Hz), 8.49 (1H, d, J = 8.8 Hz), 8.66 (1H, s). LRMS (DART+) calcd for $C_{24}H_{28}N_5O_2$ [M+H$^+$]: m/z = 418.2, found 418.2.

*2.2.3.3. N-{2-[5-(2-Methoxyethoxy)-1H-benzo[d]imidazol-1-yl]quinolin-8-yl}-N′,N′-dimethylethane-1,2-diamine (**5f**).* The title compound **5f** was afforded (145 mg, 85%) as a yellow solid. ^{1}H NMR (400 MHz, $CDCl_3$): δ 2.38 (6H, s), 2.73–2.76 (2H, m), 3.38–3.39 (2H, m), 3.50 (3H, s), 3.82–3.84 (2H, m), 4.23–4.25 (2H, m), 6.48 (1H, br s), 6.76 (1H, d, J = 8.0 Hz), 7.10–7.14 (2H, m), 7.37 (1H, d, J = 2.4 Hz), 7.40–7.44 (1H, m), 7.64 (1H, dd, J = 1.6, 8.8 Hz), 8.24–8.26 (1H, m), 8.31 (1H, d, J = 9.2 Hz), 8.60 (1H, d, J = 1.6 Hz). LRMS (DART+) calcd for $C_{23}H_{28}N_5O_2$ [M+H$^+$]: m/z = 406.2, found 406.2.

*2.2.3.4. N,N-Diethyl-N′-{2-[5-(2-methoxyethoxy)-1H-benzo[d]imidazol-1-yl]quinolin-8-yl}ethane-1,2-diamine (**5g**).* The title compound **5g** was afforded (105 mg, 52%) as a yellow solid. ^{1}H NMR (400 MHz, $CDCl_3$): δ 1.06–1.10 (6H, m), 2.65–2.70 (4H, m), 2.87–2.89 (2H, m), 3.38–3.39 (2H, m), 3.50 (3H, s), 3.82–3.84 (2H, m), 4.22–4.25 (2H, m), 6.48 (1H, br s), 6.77 (1H, d, J = 7.6 Hz), 7.10–7.12 (2H, m), 7.37 (1H, d, J = 2.4 Hz), 7.40–7.44 (1H, m), 7.65 (1H, dd, J = 1.6, 8.8 Hz), 8.19–8.24 (1H, m), 8.26 (1H, dd, J = 1.2, 8.4 Hz), 8.63 (1H, s). LRMS (DART+) calcd for $C_{25}H_{32}N_5O_2$ [M+H$^+$]: m/z = 434.2, found 434.3.

*2.2.4. General procedure for the preparation of compounds (**6a, 6b**)*

A mixture of piperidin-4-ol (610 mg, 6.0 mmol, 1.0 eq.), *N,N*-diisopropylethylamine (DIPEA) (1.6 mL, 9.0 mmol, 1.5 eq.), and di-*tert*-butyl dicarbonate (Boc_2O) (520 mg, 2.4 mmol, 0.4 eq.) in dry dichloromethane (15 mL) was stirred at room temperature for 19 h under nitrogen atmosphere. The reaction mixture was diluted with dichloromethane and washed with saturated aqueous $NaHCO_3$ and brine. The organic layer was dried over anhydrous sodium sulfate, filtered, and concentrated under reduced pressure. The residue was purified by column chromatography on silica gel (chloroform/methanol = 50/1) to afford Boc-aminoalcohol (*tert*-butyl 4-hydroxypiperidine-1-carboxylate) as a colorless solid (350 mg, 29%). The purified material (350 mg, 1.7 mmol, 1.0 eq.) was dissolved in dichloromethane (DCM) (5 mL). Triethylamine (TEA) (480 μL, 3.7 mmol, 2.2 eq.) was added to the solution and the solution was cooled to 0 °C using an ice bath. To the mixture, methane sulfonyl chloride (MsCl) (160 μL, 2.0 mmol, 1.2 eq.) was added dropwise at 0 °C. The mixture was gradually warmed to room temperature and stirred overnight. The reaction mixture was quenched by addition of water (10 mL) dropwise and extracted with DCM (3 × 20 mL). The organic layer was dried over anhydrous sodium sulfate, filtered, and concentrated under reduced pressure to obtain **6a** (280 mg) as a colorless solid. The product was used for the next step without further purification. The same procedure was performed to obtain compound **6b**.

*2.2.5. General procedure for the preparation of compounds (**7a** and **7b**)*

To a mixture of **2** (168 mg, 0.5 mmol, 1.0 eq.) and *tert*-butyl 4-[(methylsulfonyl)oxy]piperidine-1-carboxylate (223 mg, 0.8 mmol, 1.6 eq.) (**6a**) in dry toluene (5 mL) was added cesium carbonate (495 mg, 1.5 mmol, 3.0 eq.). The mixture was stirred at 100 °C for overnight under nitrogen atmosphere. After reaction completion, water was added to the mixture and the mixture was extracted using ethyl acetate (3 × 30 mL). The organic layers were collected and washed with saturated aqueous $NaHCO_3$. The organic layer was dried over sodium sulfate, filtered, and concentrated under reduced pressure. The intermediate product was obtained after purification by column chromatography on silica gel (chloroform/methanol = 100/1). TFA (1 mL) was added to the intermediate product (0.5 mmol, 1.0 eq.), and the mixture was stirred at room temperature for 15 min. After removing TFA by nitrogen gassing, the residue was dissolved in dichloromethane and washed with 0.1 M HCl. After adjusting pH to 9.0 using 0.1 M NaOH aqueous solution, the water layer was extracted using dichloromethane (3 × 25 mL). The organic layer was dried over sodium sulfate, filtered, and concentrated under reduced pressure to obtain the titled compound (**7a**). The same procedure was carried out to obtain compound **7b**.

*2.2.5.1. 2-[5-(2-Methoxyethoxy)-1H-benzo[d]imidazol-1-yl]-8-(piperidin-4-yloxy)quinoline (**7a**).* The title compound **7a** was afforded (80 mg, 40%) as a pale white solid. ^{1}H NMR (400 MHz, $CDCl_3$): δ 3.44–3.49 (4H, m), 3.50 (3H, s), 3.62–3.63 (1H, m), 3.82–3.85 (2H, m), 4.05–4.06 (4H, m), 4.23–4.26 (2H, m), 6.80 (1H, br s), 7.15–7.18 (1H, m), 7.24–7.26 (1H, m), 7.37–7.38 (1H, m), 7.40–7.54 (2H, m), 7.71 (1H, dd, J = 2.0, 8.8 Hz), 8.34 (1H, dd, J = 1.6, 8.4 Hz), 8.50 (1H, d, J = 2.4, 9.2 Hz), 8.64 (1H, d, J = 1.6 Hz). LRMS (DART+) calcd for $C_{24}H_{27}N_4O_3$ [M+H$^+$]: m/z = 419.2, found 419.2.

*2.2.5.2. cis-4-({2-[5-(2-Methoxyethoxy)-1H-benzo[d]imidazol-1-yl]quinolin-8-yl}oxy)cyclohexan-1-amine (**7b**).* The title compound **7b** was afforded (97 mg, 45%) as a pale white solid. ^{1}H NMR (400 MHz, $CDCl_3$): δ 1.62 (2H, br s), 1.72–1.74 (2H, m), 1.78–1.86 (4H, m), 2.28–2.31 (2H, m), 2.81–2.85 (1H, m), 3.50 (3H, s), 3.82–3.84 (2H, m), 4.22–4.24 (2H, m), 4.84 (1H, br s), 7.16–7.21 (2H, m), 7.35 (1H, d, J = 2.4 Hz), 7.42–7.48 (2H, m), 7.70 (1H, d, J = 8.8 Hz), 8.29 (1H, d, J = 8.8 Hz), 8.64 (1H, s), 8.86 (1H, d, J = 8.8 Hz). LRMS (DART+) calcd for $C_{25}H_{29}N_4O_3$ [M+H$^+$]: m/z = 433.2, found 433.2.

*2.2.6. 5-Iodo-2-[5-(2-methoxyethoxy)-1H-benzo[d]imidazol-1-yl]-8-(piperazin-1-yl)quinoline (**8**)*

A mixture of *N*-chlorosuccinimide (NCS) (53 mg, 0.4 mmol, 1.2 eq.) and sodium iodide (NaI) (60 mg, 0.4 mmol, 1.2 eq.) in acetic acid (5 mL) was added to **5a** (119 mg, 0.3 mmol, 1.0 eq.) in acetic acid (5 mL) and the mixture was stirred at 50 °C overnight under nitrogen atmosphere. After adjusting pH to 9.0 using saturated aqueous sodium bicarbonate ($NaHCO_3$), the reaction mixture was extracted with dichloromethane (3 × 30 mL). The organic layer was dried over sodium sulfate, filtered, and concentrated under reduced pressure. The crude product was purified by column chromatography on silica gel (chloroform/methanol = 50/1) to afford **8** (103 mg, 65%) as a pale yellow solid. ^{1}H NMR (400 MHz, $CDCl_3$): δ 2.90–2.94 (1H, br s), 3.21–3.24 (3H, m), 3.38–3.45 (4H, m), 3.50 (3H, s), 3.82–3.84 (2H, m), 4.23–4.25 (2H, m), 6.98–7.02 (1H, m, 7.16 (1H, d, J = 8.8 Hz), 7.37 (1H, s), 7.74 (1H, d, J = 8.8 Hz), 8.00 (1H, d, J = 8.4 Hz), 8.46 (1H, d, J = 8.0 Hz), 8.56 (1H, d, J = 8.0 Hz), 8.65 (1H, s). ^{13}C NMR (100 MHz, $CDCl_3$): δ 156.15, 150.39, 147.16, 145.53, 144.76, 141.23, 137.52, 129.21, 126.73, 119.41, 114.86, 114.68, 113.64, 103.67, 89.03, 71.11, 67.87, 59.29, 53.25 (2C), 51.94, 46.47 (2C). LRMS (ESI+) calcd for $C_{23}H_{24}IN_5O_2$ [M+H$^+$]: m/z = 530.1, found 530.1.

*2.2.7. tert-Butyl 4-{5-iodo-2-[5-(2-methoxyethoxy)-1H-benzo[d]imidazol-1-yl]quinolin-8-yl}piperazine-1-carboxylate (**9**)*

A mixture of **8** (103 mg, 0.2 mmol, 1.0 eq.), *N,N*-diisopropylethylamine (DIPEA) (54 μL, 0.3 mmol, 1.5 eq.) and di-*tert*-butyl dicarbonate (Boc_2O) (43 mg, 0.2 mmol, 1.0 eq.) in dry dichloromethane (3 mL) was stirred at room temperature for 3 days under nitrogen atmosphere. The reaction mixture was diluted with dichloromethane and washed successively with saturated aqueous $NaHCO_3$ and brine. The organic layer was dried over sodium sulfate, filtered, and concentrated under reduced pressure to afford **9** (76 mg) as a pale yellow solid. The product was used in the following reaction without further purification.

*2.2.8. tert-Butyl 4-{2-[5-(2-methoxyethoxy)-1H-benzo[d]imidazol-1-yl]-5-(tributylstannyl)quinolin-8-yl}piperazine-1-carboxylate (**10**)*

A mixture of **9** (45 mg, 71.5 μmol, 1.0 eq.), hexabutyldistannane (144 μL, 286 μmol, 4.0 eq.), and tetrakis(triphenylphosphine)palladium

(0) $Pd[P(C_6H_5)_3]_4$ (12 mg, 10.8 μmol, 0.15 eq.) in dry toluene (2 mL) was refluxed for 22 h under nitrogen atmosphere. After removing the catalyst by filtration through a pad of Celite® and washing with toluene, the filtrate was concentrated under reduced pressure and purified by HPLC with mobile phase system methanol (A) (with 0.05% TEA) and water (B) (with 0.05% TEA), A: 95.0 − 99.5%, 20 min using $5C_{18}$ MSII (10ID × 250 mm) column, flow rate 4 mL/min, to afford **10** (25 mg, 45%) as a pale yellow solid. ^{1}H NMR (400 MHz, $CDCl_3$): δ 0.82–0.89 (9H, m), 1.11–1.23 (6H, m), 1.25–1.41 (6H, m), 1.45 (9H, s), 1.51–1.54 (6H, m), 3.34–3.36 (4H, m), 3.50 (3H, s), 3.75–3.77 (4H, m), 3.82–3.85 (2H, m), 4.23–4.26 (2H, m), 7.15 (1H, dd, J = 2.4, 8.8 Hz), 7.21 (1H, dd, 2.4, 7.2 Hz), 7.67 (1H, d, J = 2.0 Hz), 7.60 (1H, dd, J = 2.4, 7.2 Hz), 7.72 (1H, J = 2.4, 8.8 Hz), 8.24 (1H, dd, J = 2.4, 8.8 Hz), 8.44 (1H, dd, J = 2.0, 8.8 Hz), 8.65 (1H, d, J = 2.4 Hz). ^{13}C LRMS (DART+), calcd for $C_{40}H_{60}N_5O_4Sn$ $[M+H^+]$: m/z = 794.4, found 794.5.

2.2.9. 4-{5-Iodo-2-[5-(2-methoxyethoxy)-1H-benzo[d]imidazol-1-yl] quinolin-8-yl}morpholine (11)

A mixture of NCS (53 mg, 0.4 mmol, 1.2 eq.) and sodium iodide (NaI) (60 mg, 0.4 mmol, 1.2 eq.) in acetic acid (5 mL) was added to **5b** (130 mg, 0.3 mmol, 1.0 eq.) in acetic acid (5 mL) and the mixture was stirred at 50 °C overnight under nitrogen atmosphere. After adjusting pH to 9.0 using saturated aqueous sodium bicarbonate ($NaHCO_3$), the reaction mixture was extracted with dichloromethane (3 × 30 mL). The organic layer was dried over sodium sulfate, filtered, and concentrated under reduced pressure. The crude product was purified by column chromatography on silica gel (chloroform/methanol = 50/1) to afford **11** (110 mg, 70%) as a pale yellow solid. ^{1}H NMR (400 MHz, $CDCl_3$): δ 3.39–3.41 (4H, m), 3.50 (3H, s), 3.82–3.84 (2H, m), 4.03–4.05 (4H, m), 4.23–4.25 (2H, m), 6.98 (1H, d, J = 8.0 Hz), 7.17 (1H, dd, J = 2.4, 8.8 Hz), 7.38 (1H, d, J = 2.0 Hz), 7.74 (1H, d, J = 9.2 Hz), 8.02 (1H, d, J = 8.0 Hz), 8.50 (1H, d, J = 8.8 Hz), 8.58 (1H, d, J = 9.2 Hz), 8.64 (1H, s). LRMS (ESI+) calcd for $C_{23}H_{24}IN_4O_3$ $[M+H^+]$: m/z = 531.1, found 531.1.

2.2.10. 4-{2-[5-(2-Methoxyethoxy)-1H-benzo[d]imidazol-1-yl]-5-(tributylstannyl)quinolin-8-yl}morpholine (12)

A mixture of **11** (45 mg, 85 μmol, 1.0 eq.), hexabutyldistannane (171 μL, 340 μmol, 4.0 eq.), and tetrakis(triphenylphosphine)palladium (0) $Pd[P(C_6H_5)_3]_4$ (14 mg, 12.75 μmol, 0.15 eq.) in dry toluene (2 mL) was refluxed for 48 h under nitrogen atmosphere. After removing the catalyst by filtration through a pad of Celite® and washing with toluene, the filtrate was concentrated under reduced pressure and purified by HPLC with mobile phase system methanol (A) (with 0.05% TEA) and water (B) (with 0.05% TEA), A : 97.0 − 99.5%, 20 min using $5C_{18}$ MSII (10ID × 250 mm) column, flow rate 4 mL/min, to afford **12** (29 mg, 50%) as a pale colorless solid. ^{1}H NMR (400 MHz, $CDCl_3$): δ 0.82–0.89 (9H, m), 1.11–1.23 (6H, m), 1.25–1.41 (6H, m), 1.51–1.54 (6H, m), δ 3.36–3.39 (4H, m), 3.49 (3H, s), 3.82–3.85 (2H, m), 4.02–4.04 (4H, m), 4.23–4.25 (2H, m), 6.98 (1H, d, J = 8.0 Hz), 7.17 (1H, dd, J = 2.4, 8.8 Hz), 7.38 (1H, d, J = 2.0 Hz), 7.74 (1H, d, J = 9.2 Hz), 8.22 (1H, d, J = 8.0 Hz), 8.50 (1H, d, J = 8.8 Hz), 8.58 (1H, d, J = 9.2 Hz), 8.64 (1H, s). LRMS (DART+), calcd for $C_{35}H_{51}N_4O_3Sn$ $[M+H^+]$: m/z = 695.3, found 695.3.

2.3. Cell viability assays

The cell viability assays of non-iodinated (**5a–5g**, **7a** and **7b**) and iodinated compounds (**8** and **11**) were evaluated as described previously.[35,36] Namely, TR-PCT1 cells (positive-PDGFRβ) were seeded on 96-well plates (5×10^3 cells/well) and cultured at 33 °C in DMEM medium with 20 ng/mL PDGF-BB and 2% FBS in a 5% CO_2 incubator. Cells were treated with each compound for 72 h and cell viability was determined by the Cell Counting Kit-8.

2.4. Radiolabeling

Radiolabeling of [^{125}I]**8** and [^{125}I]**11** was performed by an iodo-destannylation reaction of the corresponding tributylstannyl precursors (**10** or **12**) using NCS as an oxidizing agent. The radiotracers were isolated by RP-HPLC using a Cosmosil $5C_{18}$MSII column (4.6 ID × 150 mm) at the flow rate of 1 mL/min with a gradient mobile phase of 70% methanol in water with 0.05% TEA to 90% methanol in water with 0.05% TEA for 20 min. The column temperature was maintained at 40 °C. Radiochemical yield and purity were determined by radio-HPLC analysis.

2.4.1. Synthesis of [^{125}I]8

A solution of [^{125}I]NaI (370 kBq, 2 μL) was charged into a sealed vial containing **10** (1 mg/mL, 5 μL), acetic acid (5%, 30 μL), acetonitrile (55 μL), and NCS (5 mg/mL, 10 μL). The mixture was shaken at room temperature for 15 min, quenched by addition of sodium hydrogensulfite (5 mg/mL, 10 μL) and the solvent was removed by nitrogen gassing. TFA was added to the residue and the shaking was allowed to continue for 30 min. After removing TFA by nitrogen gassing, the residue was mixed with initial mobile phase of HPLC. The reaction mixture was shaken for some minutes, filtered, and analyzed by HPLC.

2.4.2. Synthesis of [^{125}I]11

A solution of [^{125}I]NaI in 0.1 M NaOH aqueous solution (2 μL) was added in a sealed vial containing **12** (1 mg/mL, 5 μL), acetic acid (5%, 10 μL), acetonitrile (10 μL), and NCS (5 mg/mL, 15 μL). The mixture was shaken at room temperature for 15 min, quenched by addition of sodium hydrogensulfite (5 mg/mL, 15 μL) and purified by HPLC.

2.5. Determination of partition coefficient

Partition coefficients of [^{125}I]**8** and [^{125}I]**11** into *n*-octanol and 0.1 M phosphate buffer (PB) pH 7.4 were measured as described previously with a slight modification.[39] Briefly, [^{125}I]**8** or [^{125}I]**11** was added to the mixture of *n*-octanol (3.0 mL) and PB (3.0 mL) in a test tube. The test tube was vortexed (1 min), left at room temperature (10 min), and centrifuged (5 min, 3,060*g*, 4 °C). *n*-Octanol layer (2.0 mL) was transferred into new test tube followed by addition of fresh *n*-octanol (1.0 mL) and PB (3.0 mL). After repeating vortex, standing, and centrifuging, radioactivity of each layer, *n*-octanol (1.0 mL) and PB (1.0 mL), was counted using an auto well gamma counter (n = 4). The partition coefficient was determined by calculating the ratio of radioactivity in *n*-octanol to that in PB, and expressed as a common logarithm (log *P*).

2.6. In vitro stability assay

The stability of radiotracers, [^{125}I]**8** and [^{125}I]**11**, were analyzed as described previously with a slight modification.[35,40,41] Briefly, [^{125}I]**8** or [^{125125}I]**11** solution (50 μL) in sealed tube containing 0.1 M phosphate buffered saline (PBS) pH 7.4 (450 μL) was incubated at 37 °C for 1, 3, 6, and 24 h. After incubation, the purities of radiotracers were analyzed by TLC using chloroform/methanol = 5/1 and 25/1 for [^{125}I]**8** and [^{125}I]**11**, respectively as a developing solvent and the results were confirmed by HPLC.

2.7. Cellular uptake studies

BxPC3-luc cell lines were used to perform the radiotracer uptake experiments which were cultured in RPMI 1640 medium containing 10% FBS and penicillin (100 IU/mL)-streptomycin (100 μg/mL) on 6-

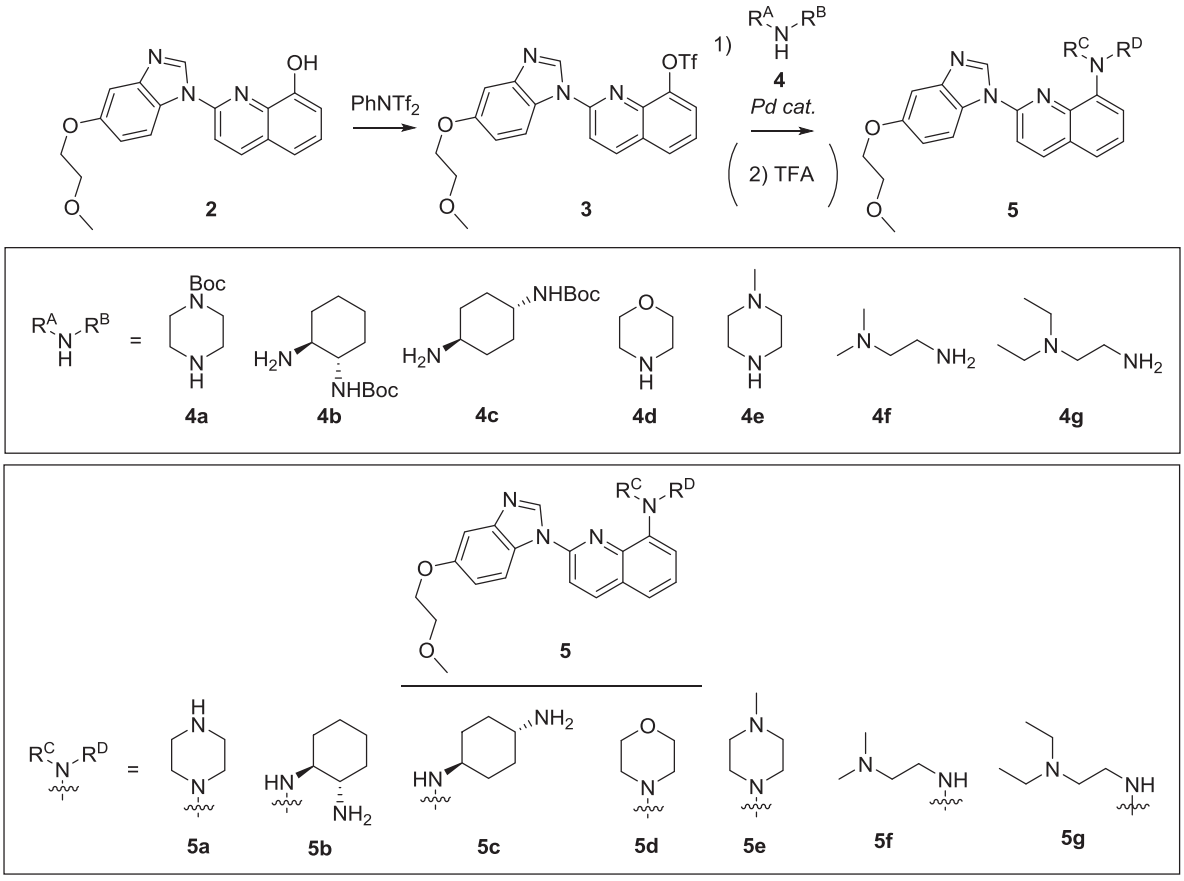

Scheme 1. Synthesis of benzo[*d*]imidazole-quinoline derivatives. *N*-phenyl-bis(trifluoromethanesulfonimide), room temperature, 2 d; 1) tris(dibenzylideneacetone) dipalladium(0), cesium carbonate, *rac*-BINAP, reflux, 3 d; 2) TFA.

well culture plates (containing 2×10^5 cells/well) for 24 h using a humidified atmosphere (5% CO_2) incubator at 37 °C.[35,42] After removal of medium, a solution of [^{125}I]**8** or [^{125}I]**11** (3.7 kBq/well) in medium without FBS was added. After incubation for 0.5, 1, 2, and 4 h, the medium from each well was removed and the cells were washed once with ice-cold PBS (1 mL). The cells were dissolved using 1 M NaOH aqueous solution (0.5 mL) and wells were washed with 1 M NaOH aqueous solution (0.5 mL). The radioactivity of pooled basic fractions

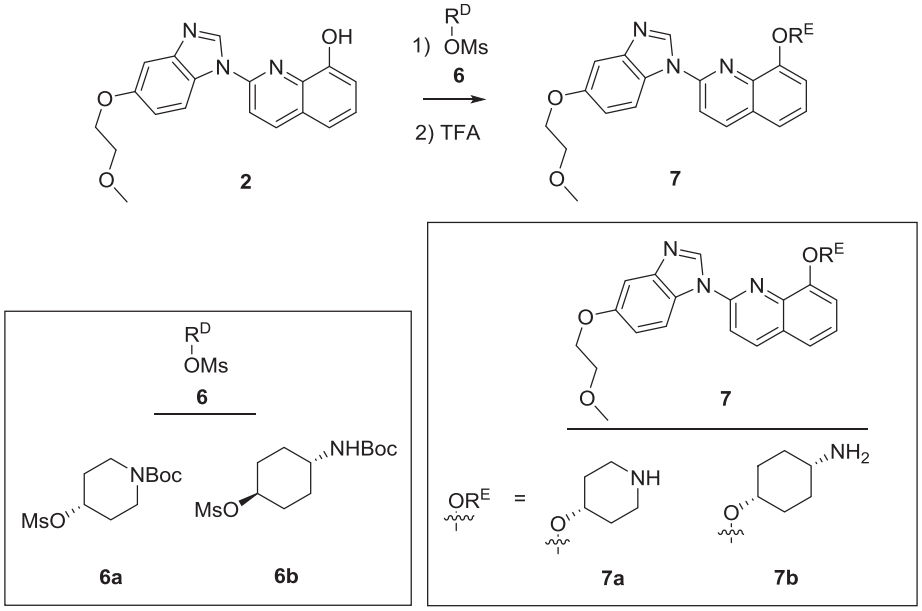

Scheme 2. Synthesis of benzo[*d*]imidazole-quinoline derivatives. 1) Cesium carbonate, reflux, overnight; 2) TFA.

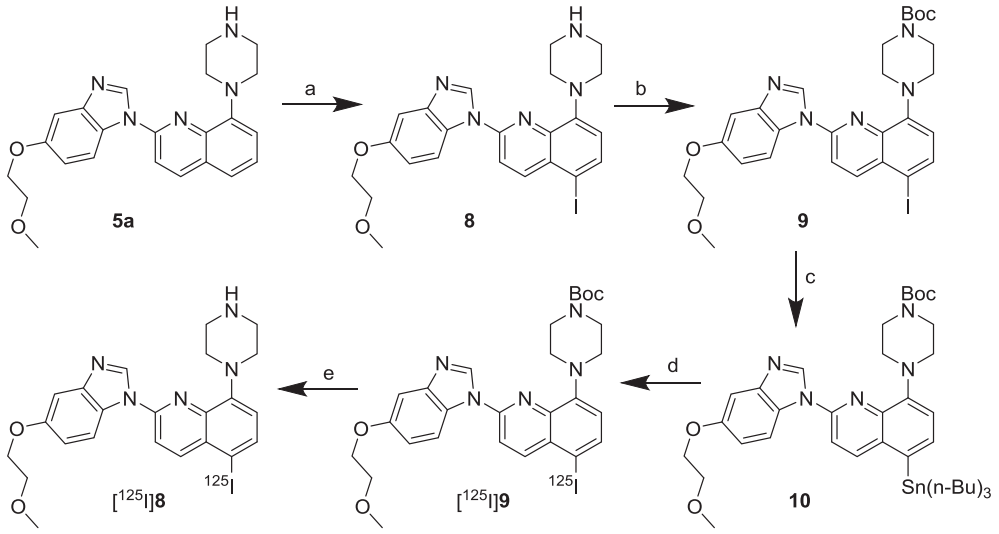

Scheme 3. Synthesis of reference compound, precursor, and radioiodinated compound [^{125}I]**8** (a) NCS, NaI, 50 °C, overnight (b) Boc_2O, TEA, room temperature, 3 d (c) hexabutyldistannane, $Pd[P(C_6H_5)_3]_4$, reflux, 24 h (d) [^{125}I]NaI, NCS, acetic acid, room temperature, 15 min (e) TFA, room temperature, 30 min.

was determined using an auto well gamma counter. The total protein in the cell was quantified using a BCA Protein Assay Kit following the manufacturer's recommendations and bovine serum albumin as a protein standard. All data were expressed as percent dose per microgram protein (%dose/μg protein).

In *in vitro* blocking experiments, inhibitors (**1**, **8**, or **11** with final concentration 10 μM) in 1 mL of medium without FBS were added to wells containing 2×10^5 cells/well. After incubation for 10 min, [^{125}I]**8** or [^{125}I]**11** (3.7 kBq/well) in 1 mL of medium without FBS was added to each well. Radioactivity and protein concentration in cells were determined using the same method above-mentioned.

2.8. Competitive binding assay

BxPC3-luc cells in RPMI 1640 medium containing 10% FBS and penicillin (100 IU/mL)-streptomycin (100 μg/mL) were seeded on 24-well plates (containing 50,000 cells/wells) and incubated for 24 h using a humidified atmosphere (5% CO_2) at 37 °C. Nine concentrations of displacing nonradiolabeled ligands (**1** and **8**) (ranging from 1 pM to 1 mM) and [^{125}I]**8** in RPMI 1640 medium without 10% FBS were incubated at 37 °C for 4 h. After the cells were washed twice with ice-cold PBS (250 μL), the unbound radioligand was removed. The cells were dissolved using 1 M NaOH aqueous solution (250 μL) and wells were washed with 1 M NaOH aqueous solution (250 μL). The bound radioactivity was determined using an auto well gamma counter.

2.9. Animals

Experiments with animals were conducted by the Guidelines for the Care and Use of Laboratory Animals of Kanazawa University. The animals were housed with free access to food and water at 23 °C with a 12 h light/dark schedule. Six-week-old male ddY (27–30 g) and four-week-old female BALB/c *nu/nu* mice (12–17 g) were purchased from Japan SLC Inc. (Hamamatsu, Japan). For preparing the tumor-bearing model, 5×10^6 BxPC3-luc cells were subcutaneously inoculated into the left shoulder of BALB/c *nu/nu* mice. The tumor reached palpable size for biodistribution experiments after two weeks of the inoculation.

2.9.1. Biodistribution study

Mice were intravenously injected via the tail with a saline solution of [^{125}I]**8** (74 kBq, 100 μL), containing 1% tween-80 and 10% ethanol. The ddY mice were sacrificed at 10 min, 1, 4, and 24 h; meanwhile, tumor-bearing mice were sacrificed at 1 h postinjection.

For *in vivo* blocking studies, tumor-bearing mice were intraperitoneally injected with 200 μL of an excess of inhibitor, **1** (40 mg/kg), 1 h before intravenous injection of [^{125}I]**8** (74 kBq, 100 μL). At 1 h postinjection of [^{125}I]**8**, the mice were sacrificed.

Tissues of interest were removed and weighed. The radioactivity of the tissues was determined using an auto well gamma counter as described-above in cellular uptake study and counts were corrected for background radiation. The data were expressed as percent injected dose per gram tissue (%ID/g).

2.10. Statistical analysis

All data were analyzed using GraphPad 5.0 software (La Jolla, CA, USA) and displayed as mean ± standard deviation (SD). Significance for *in vitro* blocking studies was calculated using a one-way analysis of variance (ANOVA) followed by Dunnett's post hoc test compared to the control group. Significance in cell viability assays was determined using ANOVA followed by Tukey's post hoc test. IC_{50} values for binding assay were calculated by nonlinear regression. Significance for *in vivo*

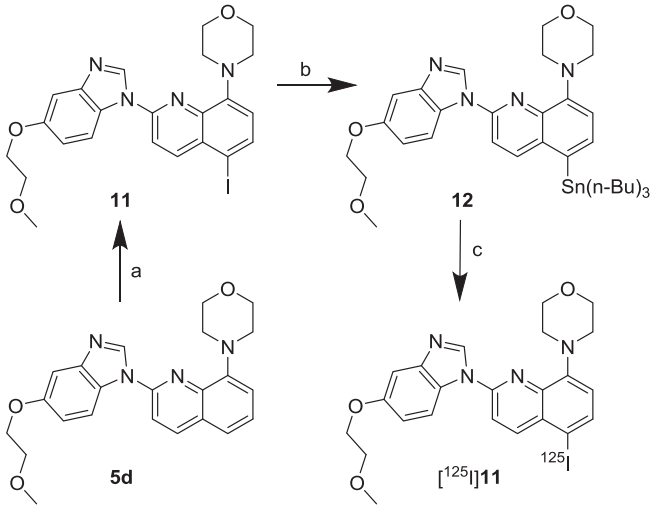

Scheme 4. Synthesis of reference compound, precursor, and radioiodinated compound [^{125}I]**11** (a) NCS, NaI, 50 °C, overnight (b) hexabutyldistannane, $Pd[P(C_6H_5)_3]_4$, reflux, 48 h (c) [^{125}I]NaI, NCS, acetic acid, room temperature, 15 min.

blocking studies between control and blocking groups were calculated using unpaired Student's *t*-test. Results were considered statistically significant at $p < 0.05$.

3. Result and discussion

3.1. Synthesis of reference compounds and precursors

The benzimidazole–quinoline derivatives **5a**–**5g**, **7a**, and **7b** were readily synthesized from the common intermediate **2**, which was synthesized according to a previously reported procedure (Schemes 1 and 2).

3.1.1. Non-iodinated compounds

The potency of benzimidazole–quinoline derivatives **5a**–**5g**, **7a**, and **7b** to reduce the viability PDGFRβ-overexpressed (TR-PCT1) cell line were evaluated. Among those derivatives compounds **5a** and **5d** exhibited more potent proliferation inhibition effects in PDGFRβ-positive cells than **1**.

3.1.2. Iodinated compounds

The iodination of **5a** and **5d** derivatives **8** and **11** were subsequently synthesized as shown in Schemes 3 and 4, respectively. Iodine was incorporated into the C-5 of the **5a** and **5b** quinoline core, using a solution of NCS and NaI in acetic acid to yield **8** and **11** (Schemes 3 and 4, respectively).

3.2. Cell viability assays

In this study the binding affinities of synthesized-compounds were evaluated using TR-PCT1 as PDGFRβ-positive cells. The PDGFRβ expressing gene of TR-PCT1 was superior to PDGFRα using PDGF-BB

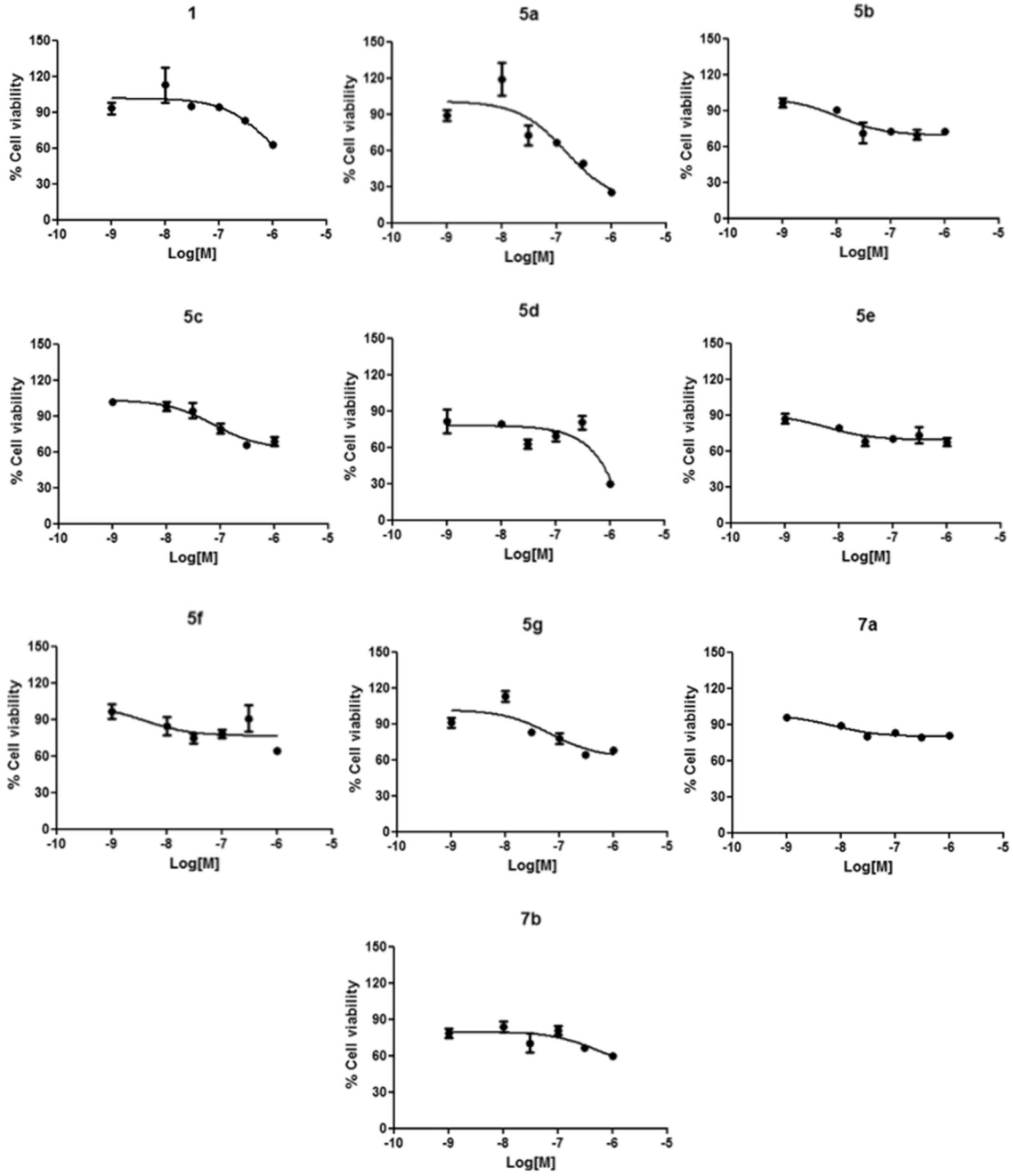

Fig. 2. Cell viability after exposure **1**, **5a**–**5g**, **7a,** and **7b** by WST-8 assay. Data were presented as mean ± SD for three samples.

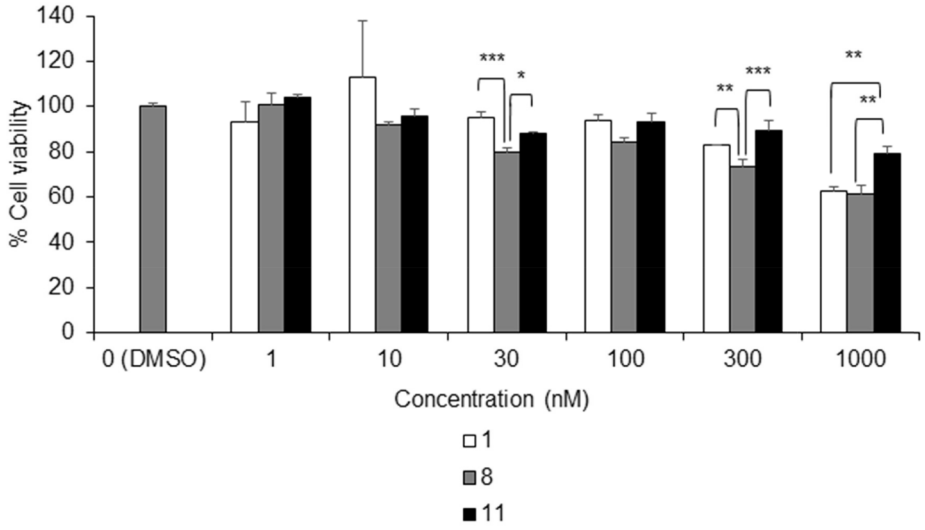

Fig. 3. Cell viability after exposure to **1**, **8**, and **11** by WST-8 assay. Data were presented as mean ± SD for three samples. Significance was determined using a one-way ANOVA followed by Tukey's post hoc test ($^{*}p < 0.05$; $^{**}p < 0.01$; $^{***}p < 0.001$).

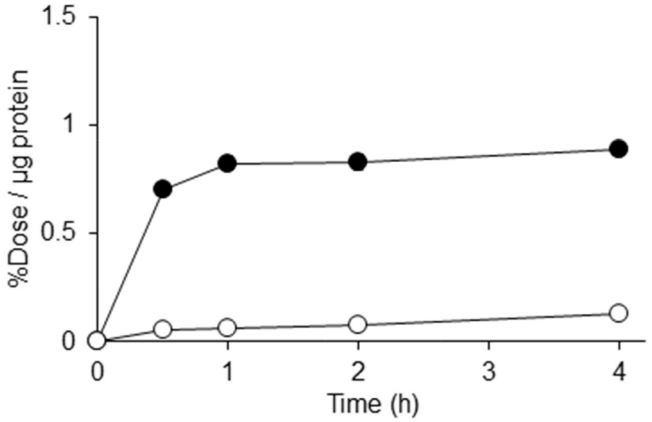

Fig. 4. Cellular uptake study. Time-dependent accumulation of [^{125}I]**8** (closed circles) and (b) [^{125}I]**11** (open circles) in BxPC3-luc cells. Data were presented as mean ± SD for three samples.

ligand, this was supported by *q*RT-PCR result (supporting information). The binding affinities of the nine non-iodinated benzimidazole–quinoline derivatives (**5a–5g** and **7a–7b**) and two iodinated derivatives (**8** and **11**) to PDGFRβ ATP-binding site were evaluated using PDGFRβ overexpressing TR-PCT1 cells. The cells were treated with 1–1000 nM of synthesized ligands, **1**, **5a–5g**, **7a–7b**, **8**, or **11**. As shown in Fig. 2, the initial SAR studies suggested that the substituent on the C-8 of the quinoline group (piperidine part) of **1** influenced the quinoline derivative affinity towards PDGFRβ. Replacing the 4-amino-1-piperidino group of **1** with cyclic secondary amino groups such as 1-piperazino (**5a**) or 4-morpholino group (**5d**) had a significant impact in reducing the viability of TR-PCT1 cells. The *N*-methylated derivative of **5a** (**5e**) exhibited lower potency. Compounds with cyclohexanediamine (**5b** and **5c**) and ethylenediamine structures (**5f** and **5g**) at the C-8 of the quinoline group were less potent towards PDGFRβ. **7a** and **7b**, which carry alkoxy substituents on the quinoline, also exhibited low potency. The secondary amino substituents on **5a** and **5d** are relatively small and present a fixed conformation compared with other substituents. These structural characteristics might contribute to improve their affinity towards PDGFRβ. Further structural studies are needed to fully clarify the effect of the substituent on the quinoline group.

Moreover, cell viability assays of iodinated **5a** (**8**) and iodinated **5d** (**11**) using PDGFRβ overexpressing TR-PCT1 cells were performed. We confirmed that the TR-PCT1 cells hardly express PDGFRα (Fig. S1). The halogen atom introduction to a small molecule potentially influences its favored molecular conformation and its affinity to the molecular target.[43] Introduction of iodine into the C-5 of **5a** and **5d** quinoline group decreased their affinities towards PDGFRβ. In contrast to **11** which significantly lost the potency of the base compound, the potency of **8** toward TR-PCT1 cell was still at the same level as **1** (see Fig. 3).

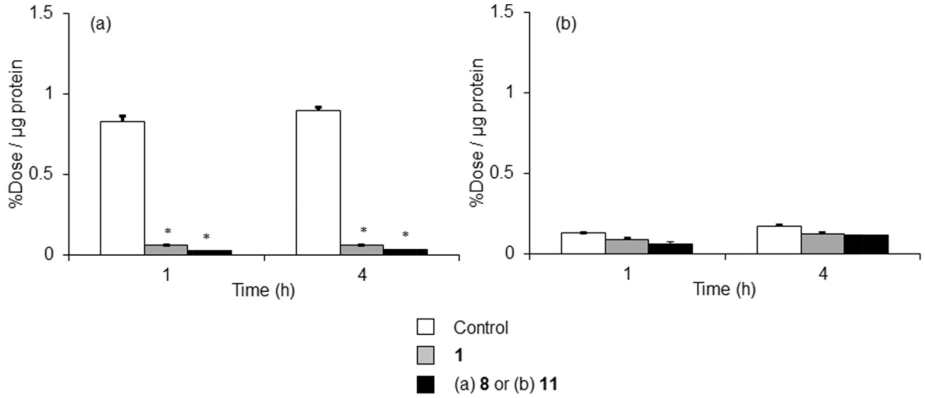

Fig. 5. In vitro blocking studies of (a) [^{125}I]**8** and (b) [^{125}I]**11** in BxPC3-luc cells. Data were presented as mean ± SD for three samples. Significance was determined using a one-way ANOVA followed by Dunnett's post hoc test ($^{*}p < 0.001$, vs control).

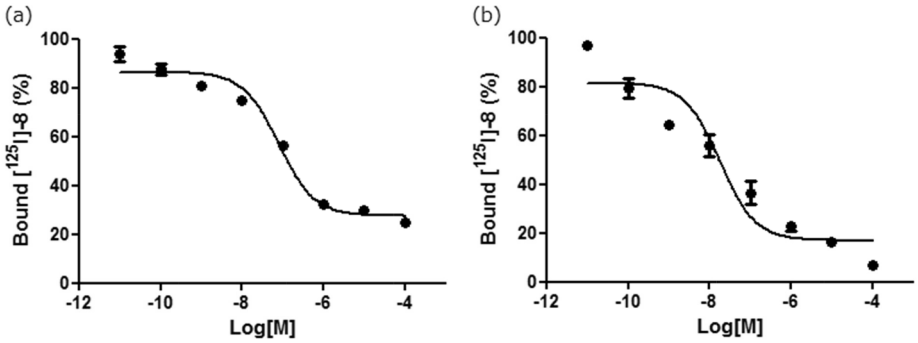

Fig. 6. Representative curves of competitive binding assay using BxPC3-luc cells. [^{125}I]**8** as a radiolabeled ligand, and a variable concentration of either (a) non-radiolabeled **1** or (b) nonradiolabeled **8** as competitors were used. Data were presented as mean ± SD for three samples.

Meanwhile, it was confirmed that compounds **8** and **11** did not have PDGFRβ-independent cytotoxicity (Fig. S2).

3.3. Radiolabeling

In the present study, we synthesized radioiodinated compounds using our previously described strategy.[35] Two novel radioiodinated derivatives of benzimidazole–quinoline were synthesized through an iododestannylation reaction with the corresponding tributyltin precursors, **10** and **12**, as outlined in Schemes 3 and 4, respectively. Both radiolabeled probes were synthesized in an acidic solution at room temperature in very high radiochemical yields (91% and 93%, respectively), using NCS as an oxidizing agent. Subsequent HPLC purification provided [^{125}I]**8** and [^{125}I]**11** with excellent radiochemical purities (> 99%).

3.4. Determination of the partition coefficient

The *n*-octanol/PB partition coefficients as log *P* values for [^{125}I]**8** and [^{125}I]**11** were 2.75 ± 0.01 and 3.56 ± 0.16, respectively, indicating that [^{125}I]**11** had a higher lipophilicity than [^{125}I]**8**.

Lipophilicity can be used to predict or rationalize *in vivo* behavior of probes, such as, membrane permeability and biodistribution. The membrane permeability of the probes is especially important because the target molecule of the probes is located in the intracellular domain. [^{125}I]**8** and [^{125}I]**11** with high lipophilicity were expected to passively penetrate cellular membrane.

3.5. In vitro stability assays

The stability of [^{125}I]**8** and [^{125}I]**11** in 0.1 M PBS (pH 7.4) was evaluated by TLC and HPLC analyses. The radiotracers' purities following a 24 h incubation at 37 °C remained 91.6 ± 0.8% for [^{125}I]**8** and 97.3 ± 0.3% for [^{125}I]**11**, respectively, revealing a good probe stability *in vitro*.

3.6. Cellular uptake studies

In vitro studies of cell uptake were performed for [^{125}I]**8** and [^{125}I]**11** using PDGFRβ-positive BxPC3-luc cells.[21,44] As shown in Fig. 4, BxPC3-luc cells exhibited a higher uptake of [^{125}I]**8**, which, in the WST-8 assay, had higher affinity against PDGFRβ than [^{125}I]**11**. Following a 4 h incubation, the cellular uptake of [^{125}I]**8** in BxPC3-luc cells reached 0.77%dose/μg protein, whereas that of [^{125}I]**11** reached only 0.17% dose/μg protein. This result was consistent with the cell viability assay, wherein **8** exhibited a higher affinity for PDGFRβ than **11** (Fig. 3).

In contrast to [^{125}I]**11**, [^{125}I]**8** uptake in BxPC3-luc cells significantly decreased after pretreatment with an excessive amount of a PDGFRβ ligand, **1**, or non-radiolabeled compounds, **8** (Fig. 5). This indicates that [^{125}I]**8** has high specificity towards PDGFRβ as a molecular target.

In the *in vitro* blocking studies, we confirmed that the blocking agents did not affect cell viability by protein assay. Protein content in each well after 4 h incubation of **1**, **8**, and control groups was 103.02 ± 2.70; 105.05 ± 3.32; and 106.48 ± 1.15 μg, respectively.

3.7. Competitive binding assay using BxPC3-luc cells

We investigated the competitive binding of [^{125}I]**8** to BxPC3-luc cells in the presence of PDGFRβ ligand, **1** and **8**. The IC_{50} values for **1** and **8** were determined to be 14 ± 4 and 75 ± 10 nM, respectively, for three independent experiments (Fig. 6).

3.8. Biodistribution studies

The biodistribution of [^{125}I]**8** in normal mice is summarized in Table 1. Following administration, high radioactivity accumulations in the liver and small and large intestines were found. Over the following 24 h, [^{125}I]**8** was mainly excreted from those tissues into feces, as confirmed by high radioactivity in the feces, indicating that the radiotracer was cleared via the hepatobiliary pathway. The results should be caused by high lipophilicity of [^{125}I]**8**. Like this excretion was usually observed in the case of small molecular probes targeting the ATP-

Table 1
Biodistribution of radioactivity at 10 min, 1, 4, and 24 h after i.v. injection of [^{125}I]**8** in ddY mice.

Tissues	Time after injection			
	10 min	1 h	4 h	24 h
[^{125}I]8				
Blood	2.06 (0.08)	0.76 (0.11)	0.33 (0.03)	0.03 (0.00)
Liver	9.85 (1.41)	3.98 (0.72)	3.12 (0.94)	0.24 (0.05)
Kidney	11.84 (0.22)	6.16 (0.32)	3.19 (0.64)	0.11 (0.02)
Small intestine	10.12 (1.21)	24.39 (2.51)	5.28 (0.95)	0.04 (0.01)
Large intestine	1.03 (0.08)	1.55 (0.28)	46.07 (8.23)	0.23 (0.05)
Spleen	5.27 (0.86)	1.34 (0.42)	0.38 (0.07)	0.03 (0.00)
Pancreas	4.19 (0.42)	2.06 (0.16)	0.70 (0.05)	0.01 (0.00)
Lung	15.74 (0.83)	4.95 (1.59)	1.52 (0.28)	0.09 (0.01)
Heart	2.78 (0.15)	0.69 (0.13)	0.20 (0.01)	0.02 (0.00)
Stomach[†]	1.73 (0.34)	2.93 (0.41)	1.10 (0.22)	0.05 (0.00)
Bone	1.42 (0.14)	0.51 (0.04)	0.17 (0.04)	0.00 (0.00)
Muscle	1.55 (0.077)	0.42 (0.08)	0.11 (0.01)	0.00 (0.00)
Brain	0.13 (0.00)	0.07 (0.01)	0.04 (0.00)	0.00 (0.00)
Urine				4.09 (0.63)
Feces				72.82 (12.18)

Data were presented as %injected dose/g tissue. Each value represent mean ± SD for three or four mice.
[†] Presented as %ID/organ.

Table 2
Biodistribution of radioactivity at 1 h after i.v. injection of [^{125}I]**8** in BxPC3-luc tumor-bearing mice.

Tissues	[^{125}I]**8**	
	Control	Blocking
Blood	0.59 (0.03)	0.70 (0.04)*
Liver	9.04 (2.89)	5.99 (0.45)
Kidney	6.99 (1.42)	8.58 (1.35)
Small intestine	44.61 (1.96)	44.82 (3.71)
Large intestine	3.35 (0.94)	3.44 (0.72)
Spleen	4.94 (1.62)	5.02 (1.02)
Pancreas	4.75 (1.66)	5.65 (0.38)
Lung	7.53 (0.26)	8.37 (0.75)
Heart	1.22 (0.29)	1.21 (0.00)
Stomach†	1.27 (0.20)	1.24 (0.09)
Bone	0.84 (0.09)	0.86 (0.09)
Muscle	0.55 (0.09)	0.58 (0.14)
Brain	0.28 (0.06)	0.31 (0.09)
BxPC3-luc tumor	1.55 (0.02)	1.19 (0.27)
Tumor/blood ratio	2.63 (0.02)	1.70 (0.11)*

Data were presented as means ± SD of %injected dose/g of tissue for three or four mice. †Presented as %ID/organ. (*$p < 0.05$ vs control [^{125}I]**8**).

binding site of receptor tyrosine kinases (RTKs).[24,31,45] Additionally, radioactivity was hardly observed in any tissues 24 h post [^{125}I]**8** injection. The low uptake levels observed in the stomach indicated that [^{125}I]**8** deiodination barely occurred *in vivo*.

The biodistribution of [^{125}I]**8** in BxPC3-luc tumor-bearing mice is summarized in Table 2. [^{125}I]**8** accumulation in the tumor 1 h post-injection was 1.55%ID/g, which is higher than that of the benzo[*d*] imidazol-quinoline derivative [^{125}I]IIQP (1.29%ID/g), used in our previous research.[35] Moreover, the tumor-to-blood ratio of radioactivity 1 h post [^{125}I]**8** injection was 2.63 ± 0.02, which was also higher than that of [^{125}I]IIQP (1.86 ± 0.34). Table 2 presents the effects of pretreatment with an excessive amount of **1** on [^{125}I]**8** biodistribution. Tumor uptake and tumor-to-blood ratio were significantly decreased by pretreatment with **1** (PDGFRβ-specific inhibitor), indicating that [^{125}I]**8** accumulation in the tumor should partly be caused by PDGFRβ. However, because the decrease was not enough, it should partly be caused by some non-specific accumulation. Even though [^{125}I]**8** should be a more promising probe to PDGFRβ than [^{125}I]IIQP, it may still be not enough to allow a clear tumor visualization. Therefore, optimized structures for higher tumor uptake and tumor-to-background ratios were required in further investigation.

4. Conclusions

The present study aimed to synthesize and evaluate several benzimidazole-quinoline derivatives, in an effort to find appropriate PDGFRβ imaging agents. The radiolabeled compounds, [^{125}I]**8** and [^{125}I]**11**, were readily synthesized from the corresponding stannylated precursors using an iododestannylation reaction with ^{125}I and NCS as an oxidizing agent. Moreover, [^{125}I]**8** was highly accumulated in PDGFRβ-positive tumors, both *in vitro* and *in vivo*. Although further structural modifications are needed for clinical applications, the results obtained in this research are useful for the design of the PDGFRβ targeting radioligands.

Conflict of interest

The authors have declared that no conflict of interest.

Acknowledgements

This work was supported in part by Grants-in-Aid for Scientific Research (16H01332, 16KT0192, 16H02668, 16H05397) from the Ministry of Education, Culture, Sports, Science and Technology, Japan.

Appendix A. Supplementary data

Supplementary data to this article can be found online at https://doi.org/10.1016/j.bmc.2018.12.016.

References

1. Broekman F, Giovannetti E, Peters GJ. *World J Clin Oncol.* 2011;2:80–93.
2. Fredriksson L, Li H, Eriksson U. *Cytokine Growth Factor Rev.* 2004;15:197–204.
3. Robson MC, Phillips LG, Thomason A, Robson LE, Pierce GF. *Lancet.* 1992;339:23–25.
4. Rodt SÅ, Åhlén K, Berg A, Rubin K, Reed RK. *J Physiol.* 1996;495:193–200.
5. Heldin CH. *Cell Commun Signal.* 2013;11:97.
6. Heldin CH. *J Neuroimmune Pharmacol.* 2014;9:69–79.
7. Ostendorf T, Eitner F, Floege J. *Pediatr Nephrol.* 2012;27:1041–1050.
8. Tamborini E, Miselli F, Negri T, et al. *Clin Cancer Res.* 2006;12:6920–6928.
9. Yang J, Liu X, Nyland SB, et al. *Blood.* 2010;115:51–60.
10. Uehara H, Kim SJ, Karashima T, et al. *J Natl Cancer Inst.* 2003;95:458–470.
11. Bedard PL, Hansen AR, Ratain MJ, Siu LL. *Nature.* 2013;501:355–364.
12. Tolmachev V, Stone-Elander S, Orlova AR. *Lancet Oncol.* 2010;11:992–1000.
13. Cornelissen B. *J Labelled Compd Radiopharm.* 2014;57:310–316.
14. Fass L. *Mol Oncol.* 2008;2:115–152.
15. Cunha L, Szigeti K, Mathé D, Metello LF. *Drug Discovery Today.* 2014;19:936–948.
16. Fretto LJ, Snape AJ, Tomlinson JE, et al. *J Biol Chem.* 1993;268:3625–3631.
17. Maudsley S, Zamah AM, Rahman N, et al. *Mol Cell Biol.* 2000;20:8352–8363.
18. Camorani S, Esposito CL, Rienzo A, et al. *Mol Ther.* 2014;22:828–841.
19. Tolmachev V, Varasteh Z, Honarvar H, et al. *J Nucl Med.* 2014;55:294–300.
20. Strand J, Varasteh Z, Eriksson O, Abrahmsen L, Orlova A, Tolmachev V. *Mol Pharm.* 2014;11:3957–3964.
21. Askoxylakis V, Marr A, Altmann A, et al. *Mol Imaging Biol.* 2013;15:212–221.
22. Marr A, Nissen F, Maisch D, et al. *Mol Imaging Biol.* 2013;15:391–400.
23. Fernandes C, Oliveira C, Gano L, Bourkoula A, Pirmettis I, Santos I. *Bioorg Med Chem.* 2007;15:3974–3980.
24. Hirata M, Kanai Y, Naka S, et al. *Ann Nucl Med.* 2013;27:431–443.
25. Kuchar M, Oliveira MC, Gano L, Santos I, Kniess T. *Bioorg Med Chem Lett.* 2012;22:2850–2855.
26. Wang JQ, Miller KD, Sledge GW, Zheng QH. *Bioorg Med Chem Lett.* 2005;15:4380–4384.
27. Wang JQ, Gao M, Miller KD, Sledge GW, Zheng QH. *Bioorg Med Chem Lett.* 2006;16:4102–4106.
28. Ishii Y, Hamashima T, Yamamoto S, Sasahara M, et al. *Pathol Int.* 2017;67:235–246.
29. Zhang Y, Gao Y, Zhang H, et al. *Blood.* 2018;131:2256–2261.
30. Newton CS, Loukinova E, Mikhailenko I, et al. *J Biol Chem.* 2005;280:27872–27878.
31. Yoshimoto M, Hirata M, Kanai Y, et al. *Biol Pharm Bull.* 2014;37:355–360.
32. Yeh HH, Ogawa K, Balatoni J, et al. *PNAS.* 2011;108:1603–1608.
33. Papaetis GS, Syrigos KN. *BioDrugs.* 2009;23:377–389.
34. Xi Y, Chen M, Liu X, Lu Z, Ding Y, Li D. *Onco Targets Ther.* 2014;7:1215–1221.
35. Effendi N, Ogawa K, Mishiro K, et al. *Bioorg Med Chem.* 2017;25:5576–5585.
36. Effendi N, Mishiro K, Takarada T, et al. *Sci Rep.* 2018;8:10369.
37. Roberts WG, Whalen PM, Soderstrom E, et al. *Cancer Res.* 2005;65:957–966.
38. Asashima T, Iizasa H, Terasaki T, et al. *Eur J Cell Biol.* 2002;81:145–152.
39. Ogawa K, Kanbara H, Shiba K, et al. *EJNMMI Res.* 2012;2:54.
40. Ogawa K, Shiba K, Akhter N, et al. *Cancer Sci.* 2009;100:2188–2192.
41. Ogawa K, Kanbara H, Kiyono Y, et al. *Nucl Med Biol.* 2013;40:445–450.
42. Ogawa K, Mizuno Y, Washiyama K, et al. *Nucl Med Biol.* 2015;42:875–879.
43. Auffinger P, Hays FA, Westhof E, Ho PS. *PNAS.* 2004;101:16789–16794.
44. Chung HW, Wen J, Lim JB, Bang S, Park SW, Song SY. *Int J Radiat Oncol Biol Phys.* 2009;75:862–869.
45. Zhang MR, Kumata K, Hatori A, et al. *Mol Imaging Biol.* 2010;12:181–191.